Geomorphology 417 (2022) 108444

Contents lists available at ScienceDirect

Geomorphology

journal homepage: www.journals.elsevier.com/geomorphology

Modeling the relative morphodynamic influence of vegetation and large wood in a dryland ephemeral stream, Arizona, USA

Julianne Scamardo [a,*], Peter A. Nelson [b], Mary Nichols [c], Ellen Wohl [a]

[a] Department of Geosciences, Colorado State University, Fort Collins, CO 80523, United States
[b] Department of Civil and Environmental Engineering, Colorado State University, Fort Collins, CO 80523, United States
[c] USDA-Agricultural Research Service Southwest Watershed Research Center, Tucson, AZ 85719, United States

ARTICLE INFO

Keywords:
Ephemeral stream
Drylands
Large wood
Sediment dynamics
Flash flood

ABSTRACT

Compared to perennial streams, studies investigating the impact of large wood on sediment transport and river corridor morphology in ephemeral streams are lacking. Due to the flashy nature of ephemeral flow regimes, opportunities to directly investigate the influence of wood in ephemeral channels are limited. Additionally, given prior studies showing a strong association between existing riparian vegetation and large wood deposition in ephemeral streams, the geomorphic impact of wood is entangled with that of vegetation. Here, we develop a hydro-morphodynamic model to investigate changes to channel and floodplain morphology due to wood and vegetation in an ephemeral stream in southeastern Arizona, USA. Three scenarios are modeled: the actual configuration of the river corridor; an experiment in which jams are removed; and an experiment in which vegetation is removed. Both large wood and vegetation effectively confined flow to the main, unvegetated channel, which became wider and deeper over the course of a single moderate flood. When isolating the impact of large wood, model results show that wood enhances channel change created by vegetation, resulting in ±0.1 to 0.3 m of additional scour or aggradation. The simulated removal of vegetation resulted in more channel change than the removal of wood alone, partially because vegetation occupies a much greater area within the stream corridor than large wood. We propose a conceptual framework where large wood could mediate sedimentation as well as the recruitment and growth of vegetation in ephemeral streams, contributing to the evolution of ephemeral stream morphology over time.

1. Introduction

The ecologic and geomorphic influence of organic matter accumulations has been readily established in perennial rivers (Montgomery et al., 2003; Gurnell, 2013; Ruiz-Villanueva et al., 2016; Wohl and Scott, 2017; Wohl, 2017; Swanson et al., 2021). Large wood (LW; >10 cm in diameter and 1 m in length) and coarse particulate organic matter (CPOM; >1 mm in diameter) can significantly impact the morphology and function of river corridors (including the channel, floodplain, and hyporheic zone (Harvey and Gooseff, 2015)). In-channel LW pieces and accumulations (i.e., jams) can increase hydraulic resistance (Curran and Wohl, 2003; MacFarlane and Wohl, 2003), which lowers local and reach-averaged velocity (Shields and Smith, 1992; Manners et al., 2007). As a result, LW can pond water (Gurnell et al., 2005; Klaar et al., 2009) and sediment upstream of jams (Bilby, 1981; Nakamura and Swanson, 1993; Faustini and Jones, 2003; Short et al., 2015). Sedimentation can aggrade the channel and encourage secondary channels to form on the floodplain (Abbe and Montgomery, 2003; Montgomery and Abbe, 2006). Channel-spanning LW jams can transform reaches from homogeneous, single-threaded channel planforms to multi-threaded planforms with a greater diversity of channel widths and depths (Wohl, 2011). Sedimentation downstream of individual LW pieces and jams can form new islands or stabilize pre-existing islands (Gurnell et al., 2005). In reaches with erodible banks and substrate, LW can cause bank and bed scour (Keller and Swanson, 1979), which can encourage lateral channel migration (Nakamura and Swanson, 1993; Lassettre et al., 2008). Although understudied compared to in-channel wood, LW on perennial floodplains can cause high sedimentation rates and spatially heterogeneous deposition during overbank flow (Jeffries et al., 2003). LW jams buried on floodplains can create hard points that resist erosion and promote avulsion and multi-threaded planforms (Collins et al., 2012). LW can be deposited in association with vegetation

* Corresponding author.
E-mail address: j.scamardo@colostate.edu (J. Scamardo).

https://doi.org/10.1016/j.geomorph.2022.108444
Received 18 April 2022; Received in revised form 5 September 2022; Accepted 6 September 2022
Available online 16 September 2022

(e.g., Lininger et al., 2021), thus creating similar increases in roughness, but the body of literature outlining the geomorphic effects of LW establishes that jams play a distinct role in shaping channels and floodplains in perennial river corridors.

In contrast, the effects and benefits of LW and CPOM in streams with ephemeral flow regimes are relatively understudied (Wohl, 2017), particularly in dryland regions where flow is predominantly controlled by high-intensity, irregular storms. A limited number of studies have quantified the volume of LW and CPOM in dryland ephemeral streams in Australia (Graeme and Dunkerley, 1993; Dunkerley, 2014), the Mediterranean (Galia et al., 2018; Galia et al., 2019; Galia et al., 2020), Africa (Jacobson et al., 1999) and the southwestern United States (Wohl et al., 2018; Wohl and Scamardo, 2022). Most studies found that LW was present but at lower volumes than in perennial rivers, and that LW and CPOM accumulations were commonly associated with existing vegetation in the ephemeral channel and floodplain (Dunkerley, 2014; Galia et al., 2020; Wohl and Scamardo, 2022). Despite the growing recognition of LW in ephemeral channels, the impact that LW and CPOM accumulations have on ephemeral stream channel morphology is still poorly constrained and, given common trapping locations, entangled with the geomorphic effect of vegetation. LW jams have rarely been observed during a flow event due to the infrequency and brevity of discharge in dryland ephemeral channels. The current understanding of how LW jams alter hydraulics during flow is based on sediment deposition patterns around jams post-flood. Significant sediment deposition has been found downstream of LW jams (Jacobson et al., 1999; Dunkerley, 2014; Galia et al., 2018), suggesting potential decreased velocity or eddying behind stable jams during flash floods. Jacobson et al. (1999) found that recent sediment accumulations acted as 'nursery bars' that could develop into elongate islands if not removed by subsequent high flows. Due to sedimentation and flow deflection, LW jams may create multi-threaded planforms in ephemeral channels (Graeme and Dunkerley, 1993; Dunkerley, 2014). However, despite some evidence that LW accumulations can affect flow paths, sedimentation, and channel morphology in dryland ephemeral streams, evidence for physical effects from LW accumulations can be unclear. Galia et al. (2018), for example, noted sediment deposition downstream from LW jams but found no scour, temporary dammed pools, or evidence of flow deflection around LW jams, suggesting that LW accumulations may have limited physical effects. As in perennial streams, LW deposition can be correlated to vegetation density in ephemeral streams (e.g., Wohl and Scamardo, 2022), because stable vegetation provides ample trapping locales for LW and CPOM. Vegetation similarly increases roughness along ephemeral channels, which can lead to sediment deposition (Nepf, 1999) and the creation or maintenance of braided planforms (Graeme and Dunkerley, 1993; Wende and Nanson, 1998). Therefore, the question remains, how do LW jams influence channel morphology in ephemeral rivers and how does the influence of LW compare to that of vegetation?

Given the difficulty of obtaining direct measurements during infrequent and short-duration flash floods, we approach this question using indirect methods. Our primary objective is to numerically model reach-scale morphological changes during a flash flood in an ephemeral stream using three scenarios: a calibrated model representing the actual configuration of the river corridor; a numerical experiment in which jams are removed; and a numerical experiment in which vegetation is removed. This allows us to compare the modeled geomorphic changes associated with the presence of LW versus those associated with vegetation and thus infer the relative importance of LW and vegetation to channel change during a flood. Given the correlation between the trapping of wood and presence of vegetation, we intend not to contrast the morphological influence of both factors, but rather to compare. We hypothesize that LW jams and vegetation will result in similar spatial patterns and magnitudes of changes in morphology, such as increased sedimentation on the floodplain and the formation of braided channels. However, we expect floodplain sedimentation and channel erosion to be greater with the inclusion of jams than without. We use two-dimensional hydro-morphodynamic models to simulate and isolate the influence of LW jams and vegetation in an ephemeral stream in southeastern Arizona.

2. Regional setting

Walnut Gulch Experimental Watershed (WGEW) encompasses ~150 km^2 of the semi-arid transition zone between the Sonoran and Chihuahuan deserts in southeastern Arizona (Fig. 1). Headwaters to Walnut Gulch start in the Dragoon Mountains and Tombstone Hills, eventually joining the San Pedro River as an ephemeral tributary. Runoff events in Walnut Gulch predominantly occur due to late summer monsoon rainfall. Bedrock in the headwaters of WGEW is primarily highly erodible Gleeson Quartz Monzonite, soft tuffs of the lower S O Volcanics Group, and sandstones and limestones of the Bisbee and Naco Groups (Osterkamp, 2008). Lowland hillslopes are underlain by the Gleeson Road Conglomerate, while river corridors are composed of late Holocene alluvium.

WGEW has been managed by the U.S. Department of Agriculture Agricultural Resources Service (USDA-ARS) since 1959. The experimental watershed was initially created to investigate the influence of upland conservation on downstream water supply. Accordingly, a series of in-channel flumes have been maintained in WGEW since the 1950s to record temporary flows. A total of 11 critical-depth flumes, specially designed to withstand intense flash floods in the watershed, record water depth and discharge of all runoff events that produce flow above a minimum threshold stage (0.003 m at small flumes, 0.015 m at large flumes) (Smith et al., 1981). Currently, flow depth is recorded using a potentiometer and converted to discharge using a known stage-discharge relationship developed for each flume.

The following study focuses on a ~2.3 km reach of WGEW immediately upstream of Flume 1, the downstream-most and largest flume in WGEW (Fig. 1). The reach is separated into two parts: the upstream-most 1.1 km, termed the study reach, and the downstream-most 1.2 km. The study reach is unconfined (average floodplain width = 115.3 m) with an anastomosing planform, while the downstream reach is more confined (average floodplain width = 46.5 m) with a single channel. The field study and interpretation of the results are limited to the study reach, but combined, the two reaches form the modeled area. The main ephemeral channel through the modeled area is largely unvegetated and consists of fine sand to medium gravel, with an average channel width of 18.1 m and average gradient of 0.01 m/m. Bedforms are not evident throughout the reach. Occasional bedrock outcrops ~5–10 m in length occur on outer meander bends in the downstream reach, but otherwise, bedrock outcrops or large (>0.5 m) boulders are rare in the channel. Approximately 31 % of the floodplain is vegetated with Arizona walnut (*Juglans major*), mesquite (genus *Prosopis*), and netleaf hackberry (*Celtis laevigata*) as well as shrubs such as Mormon tea (*Ephedra nevadensis*) and rabbitbrush (genus *Chrysothamnus*) (Fig. 2). Ground cover of grasses and sedges is limited.

3. Methods

3.1. Field data collection

A comprehensive survey of all LW and CPOM jams within the study area was conducted in August 2020. Surveys were completed by walking the extent of the study reach and documenting the location of all jams larger than 0.5 m in two principal directions (length, width, height) using a handheld Garmin GPS (accuracy ±3 m). We chose to include CPOM accumulations meeting the size requirement due to the prevalence of woody accumulations that did not meet the definition of LW, but still likely persist for years (Wohl and Scamardo, 2022). The longevity of LW and CPOM accumulations has not explicitly been monitored in WGEW, but occupation of jams by packrats and colonization by vegetation suggests that some of the surveyed jams had

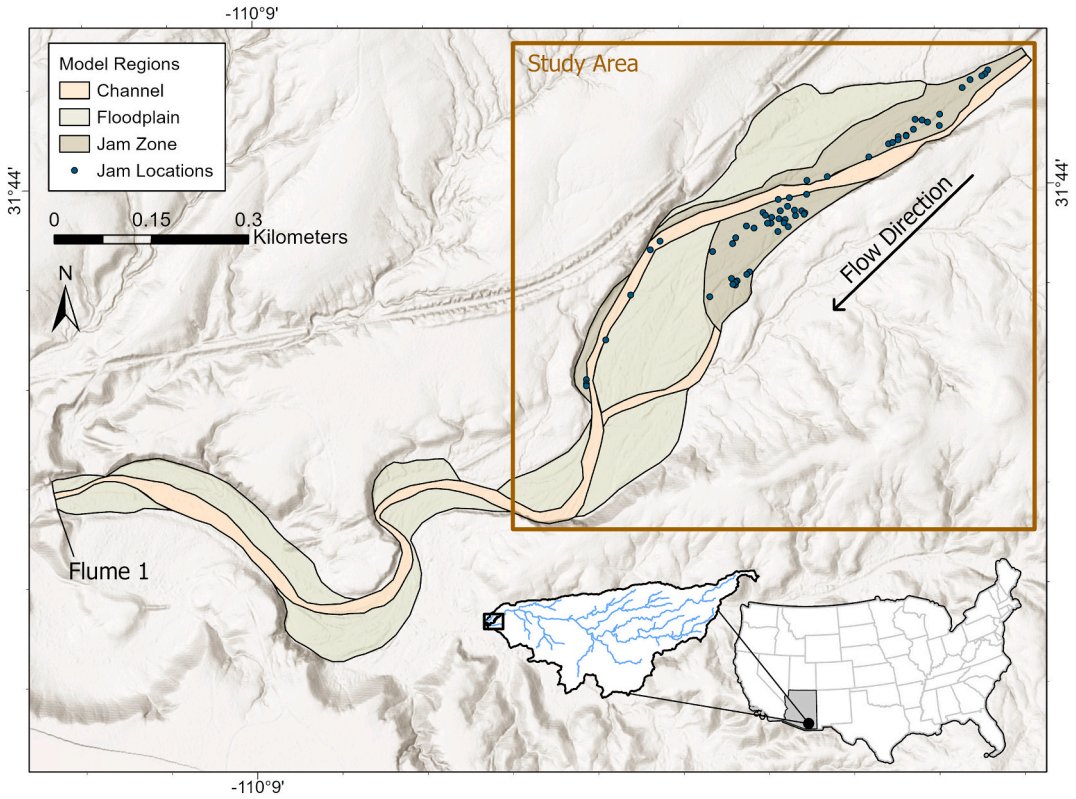

Fig. 1. Site map of the study area (box) and modeled area (colored regions) in Walnut Gulch Experimental Watershed, Arizona. Surveyed jam locations are indicated with points.

Fig. 2. Oblique aerial image of the upstream portion of the study area, showing a sparsely vegetated floodplain, multiple channels, and outcropping bedrock. Reach and floodplain boundaries are highlighted with a dashed yellow line. Camera angle is looking upstream. (For interpretation of the references to color in this figure legend, the reader is referred to the web version of this article.)

persisted for multiple seasons. Additionally, wood decay rates in dryland floodplains are low, on the order of decades to centuries, suggesting that non-mobilized wood (including large wood and CPOM) surveyed in the floodplains would persist from year-to-year (Anderson et al., 2016). Moving from upstream to downstream in the reach, we walked a series of perpendicular transects across the floodplain and channel to capture all jams. In addition to location, we measured the bounding dimensions and estimated porosity within those bounds by visually approximating the volume of void space within the jam volume (Livers et al., 2020). The occurrence and size of all LW pieces were measured within each surveyed jam and it was noted whether jams were trapped on vegetation. Finally, the location of the jam was categorized into one of four geomorphic units: main channel, secondary channel, floodplain, or bar.

Sediment cores were collected at randomly generated point locations

in the channel and floodplain within the study area to characterize grain size in the reach. Eight cores were collected in the channel and ten cores were collected on the floodplain. Cores were taken to a depth of 20 cm using a slide-hammer corer, and sediment extracted from the cores was sieved for grain size. Cores were unconsolidated and not vertically stratified post-collection; however, no armoring or noticeable vertical variation in grain sizes were noted.

3.2. Modeling domain set-up

We used SRH-2D, a two-dimensional depth-averaged hydro-morphodynamic model (Lai, 2010), to simulate a specific runoff event that occurred on 28 July 2017, starting at 6:20 PM with a peak discharge of ~96 m^3/s (Fig. S1). The 2017 event represents the largest flow recorded in the decade prior to the 2020 wood survey and has an 8-year recurrence interval based on the period of record at Flume 1. Given the magnitude and recurrence interval of the runoff event, we expect all surveyed jams to have been deposited prior to or at the front of the 2017 flood.

Model pre- and post-processing was performed using SMS 13.1 software (Aquaveo, commercial surface-water model system, https://www.xmswiki.com/wiki/SMS:SMS). A computational mesh was created by specifying the number of bounding nodes on the floodplain, channel, and jam zone boundaries. The boundaries between the floodplain and channel zones were determined from field mapping and aerial imagery. The jam zones are identified as areas of concentrated jam deposition, and boundaries were determined by the field-based wood survey (Fig. 1). The model boundaries and mesh were extended beyond the study reach to include Flume 1, to take advantage of a known outflow for model calibration. In total, the mesh contained 52,959 quadrilateral and triangular elements with an average element length of 3.1 m. Mesh element shape and size were chosen based on the need for an accurate solution while balancing increasing computational demands. Channel areas were modeled using quadrilateral elements with an average cell size of 2.5 m in the downstream and lateral directions, while floodplain areas were modeled using triangular elements with an average cell size of 2.5 m near the channel and 5.0 m near the model boundaries. The decision to vary mesh resolution across the domain was made to increase accuracy in places of expected high change, such as the channel and surrounding jam zones, while balancing computational efficiency.

Elevation was assigned to the mesh using a 1-m resolution digital elevation model (DEM) derived from airborne laser swath mapping (Heilman et al., 2008) in WGEW in 2015. We assume that minor floods between 2015 and 2017 minimally changed topography, so that the 2015 DEM represents pre-flood morphology. Sediment characteristics within the mesh domain were estimated from the sieved sediment cores taken from the bed and floodplain of the study reach. The channel was modeled with $D_{16} = 0.5$ mm, $D_{50} = 1.85$ mm, and $D_{84} = 8.8$ mm, representing medium sand to fine gravel. The floodplain and jam zones were modeled with $D_{50} = 0.7$ mm and $D_{84} = 1.6$ mm, representing coarse sand.

3.3. Hydrodynamic set up and calibration

An unsteady hydrodynamic model was developed using the hydrograph from the July 2017 runoff event in SRH-2D, which solves the depth-averaged St. Venant equations using an implicit scheme (Lai, 2010). Discharge was measured at the downstream end of the reach at Flume 1. We used an iterative process to infer an inlet hydrograph based on the outlet hydrograph. Initially, the outlet hydrograph was used as an inlet hydrograph, and the modeled outlet hydrograph was compared to the measured outlet hydrograph. The difference between the modeled and measured outlet hydrographs at each timestep was then added to the inlet hydrograph until the lowest root mean square error (RMSE) was achieved between the modeled and measured outlet hydrographs. RMSE was determined by calculating the error between the modeled and measured outlet hydrograph at each time step, in order to capture error in the magnitude and timing of discharge. Hydrograph calibration was conducted using Manning roughness values of $n = 0.036$ for the channel, $n = 0.06$ for the floodplain, and $n = 0.09$ for the jam zone, based on previously published values in Walnut Gulch (Bunch and Forbes, 2019; Michaelides et al., 2018) and additive methods for calculating roughness (Cowan, 1956). The flow outlet was modeled as a supercritical boundary to mimic the conditions immediately upstream of the critical-depth flume. For all runs, the initial bed condition was set to dry in order to mimic the conditions prior to the runoff event.

3.4. Roughness parameterization and sensitivity analysis

Model sensitivity to surface roughness was tested by varying Manning's n values in the channel, floodplain, and jam zone within a reasonable range. Previous studies in other reaches of WGEW estimated roughness values of $n = 0.027$ in the channel (Bunch and Forbes, 2019) and of $n = 0.056$ on the floodplains and hillslopes (Michaelides et al., 2018). Although published roughness values were not estimated for the study and modeled reach, they provide context for developing a reasonable range of roughness values. A range of roughness values for the channel was determined using the additive method of Cowan (1956),

$$n = (n_b + n_1 + n_2 + n_3 + n_4)m \quad (1)$$

where n_b is a base roughness value of a straight, uniform, smooth channel in natural materials, n_1 is a correction factor for surface irregularities, n_2 is a value accounting for fluctuations in cross-section shape, n_3 is a value estimating obstructions, n_4 accounts for roughness of vegetation, and m is a correction factor for meandering. A base value of $n_b = 0.025$ for coarse sand bed channels was used. The channel through the model reach is fairly uniform, with minor vegetation and obstructions. Therefore, the lower limit of channel roughness was determined to be the base value, while the upper limit of channel roughness was estimated to be $n = 0.036$ based on moderate irregularities, moderate cross-section variability, negligible obstructions, and small amounts of vegetation.

Reasonable roughness values for the floodplain were estimated using Eq. (1) adjusted for floodplains (Arcement and Schneider, 1989). The floodplain along Walnut Gulch is characterized by minor to moderate topographic irregularities (rises and sloughs) and minor to moderate brushy vegetation. A lower limit of roughness in the floodplain was determined to be $n = 0.042$, based on minor irregularities, negligible obstructions, and small amounts of vegetation. An upper limit of $n = 0.063$ was chosen, representing moderate irregularity, minor obstructions, and moderate amounts of vegetation.

Roughness for the modeled jam region, or region where the majority of jams were accumulated, was determined based on the calibrated roughness for the floodplain, given that jams were mostly accumulated in vegetated floodplain areas. In perennial systems, increasing the surface roughness value within a model is a common approach to modeling jams (Addy and Wilkinson, 2019). Accordingly, based on the floodplain roughness value, the effect of obstructions (n_3) was increased to minor or appreciable ($n = +0.01–0.03$). This increased roughness accounts for the added obstruction within the cross-section created by LW and CPOM accumulations.

Sensitivity to roughness was tested by adjusting Manning's n values for each model region within the range of realistic n-values and then comparing the RMSE of the measured and modeled hydrographs (Fig. S2). The sensitivity analysis was conducted to determine how important relative uncertainty in roughness values is on the results of the hydrodynamic model. Roughness values used in the hydrograph calibration were chosen from within the reasonable range of values for each model region, based on site characteristics and previously

published values determined upstream in the catchment. However, roughness was not explicitly calibrated due to limited available data, given that stage measurements were only conducted in one location – Flume 1 – during the duration of the flow.

3.5. Morphodynamic set up and calibration

Following the hydrograph calibration, the hydrodynamic model was then coupled with a mobile bed morphodynamic model in SRH-2D. We modeled bedload transport using both the Engelund and Hansen (1972) total load and Meyer-Peter and Muller (1948) bedload transport equations to test output sensitivity to transport equations. Both equations have been used to successfully and accurately model sediment transport and morphodynamic change in sand to gravel bed ephemeral channels (Lotsari et al., 2018; Scott, 2006). Adaptation length was modeled using the Philips-Sutherland saltation length formula, which is recommended for sand bed channels (Lai, 2020). Active layer thicknesses between 1.0 and 3.0 times the D_{90} thickness were tested to calibrate sediment transport. Sediment concentration at the inlet was estimated by calculating the transport capacity across the upstream boundary.

Six model runs were developed to calibrate the sediment equation and active layer thickness (Table S1). Resulting erosion and sedimentation from each model run were compared to a DEM of difference (DoD) for the reach between 2015 and 2018 created using the Geomorphic Change Detection Software (Wheaton et al., 2010). Although smaller flows before and after the 2017 runoff event likely changed topography within the reach, the 2017 runoff event marks a large flood during this period, and likely created a significant amount of channel change during the time of interest. Output rasters of modeled erosion and sedimentation were compared to the DoD using RMSE (Fig. S3, S4). The Engelund-Hansen sediment transport equation with an active layer twice the thickness of the D_{90} produced the lowest error and was therefore used as the calibrated model for comparisons.

3.6. Numerical experiments

Our analysis compares three morphodynamic modeling simulations: a baseline (calibrated) model including channel, vegetation, and jam zones; a model without jams, and a model without jams or vegetation. Based on the roughness sensitivity analysis, the baseline model used Manning's n values of 0.036 for the channel zone, 0.06 for vegetation zones, and 0.09 for jam zones. In the second simulation, the additional roughness of jams was removed by assigning a Manning's n value of $n = 0.06$ to the jam zones instead of $n = 0.09$; that is, jam zones were treated as floodplain zones in the model. In the third simulation, the roughness of vegetation was artificially removed by assigning a roughness value of $n = 0.036$ to both the floodplain and jam zones; that is, the entire domain was modeled using the channel roughness. Beyond roughness, all parameters of the experimental runs matched those of the calibrated model. Experimental runs were compared to the calibrated run, and were not validated or calibrated, given that the conditions being modeled were not present in the reach during the 2017 runoff event.

4. Results

4.1. Jam characteristics

A total of 61 jams were surveyed within the study area. The average volume of LW and CPOM per jam was 0.97 m^3, with the largest jam having a wood volume of 18.48 m^3 (Table 1). A total wood volume of 67.1 m^3 was recorded in the study reach, which covered 120.3 m^2 or ~0.1 % of the total study area. Jams were largely deposited on vegetation (91 % of all jams) outside of the channel region. Approximately 94 % of the measured jams were found within the denoted 'jam regions' in the model, with the remaining 6 % located in the channel wrapped around mid-channel vegetation (Fig. 3B). We observed coarse sediment deposition associated with jams (Fig. 3).

Table 1
Jam characteristics within the study reach.

Characteristic	Value
Total number of jams	61
Jams per hectare	4.1
Number of jams with LW	19
Median volume	0.51 m^3
Standard deviation of volume	2.4 m^3
Max volume	18.48 m^3
Proportion in channel	0.06
Proportion in secondary channel	0.16
Proportion in floodplain	0.67
Proportion on bar	0.11
Proportion with vegetation	0.91

4.2. Sensitivity to roughness

The model was most sensitive to roughness adjustments in the channel region, compared to the floodplain and jam zones (Fig. S3). RMSE ranged from 6.01 to 8.64 m^3/s (2.62 m^3/s range) when roughness in the channel region was varied (range of $n = 0.025$–0.036), compared to a 1.4 m^3/s range when floodplain roughness was varied (range of $n = 0.042$–0.063), and 0.9 m^3/s range when the jam zone roughness was varied (range of $n = 0.07$–0.09). Generally, RMSE was lower as roughness increased, but overall, the model is only mildly sensitive to uncertainty in roughness, as is indicated by small ranges of RMSE (1.0–2.0 m^3/s) relative to the magnitude of peak discharge (~90 m^3/s).

4.3. Modeled hydrologic characteristics

The modeled flash flood peaked 2 h after the start of the flood, similar to the measured runoff that occurred in the reach (Fig. S1). At the runoff peak, the calibrated hydro-morphodynamic model (including jams and vegetation) showed inundation across the majority of the floodplain, with high velocities confined to the main channel (Fig. 4A). Average velocity in the channel was 2.46 m/s, compared to average velocities of 0.86 m/s and 0.93 m/s in the floodplain and jam regions, respectively (Table 2). The total wetted area at the peak discharge was ~182,200 m^2 (87% of total area).

Artificially removing the roughness of jams resulted in minimal change to hydrologic conditions during the modeled runoff event (Fig. 4B). In the experiment excluding jam roughness, ~179,900 m^2 (86% of total area) of floodplain and channel were inundated. High velocity flow was still mostly confined to the channel, with an average velocity of 2.46 m/s, compared to average velocities of 0.85 m/s and 1.19 m/s in the floodplain and jam regions, respectively (Table 2). Velocity distributions and inundation are very similar to the modeled run with jams.

In contrast, the no-vegetation experiment resulted in a larger change in hydrologic conditions (Fig. 4C). Average velocity at peak inundation in the channel was 2.37 m/s, and average velocities in the floodplain and jam zones were 1.16 m/s (35 % higher than the calibrated model) and 1.62 m/s (74 % higher than the calibrated model), respectively (Table 2). Higher velocities in the floodplain and jam zones were also accompanied by higher standard deviations in velocity compared to the calibrated run and no-jam experiment, reflecting concentrated high-velocity areas in side-channels on the floodplain and jam zones. Higher floodplain velocities were coupled with a slightly smaller inundated area of 173,500 m^2 (83% of total area).

4.4. Modeled erosion and deposition

Significant deposition occurred at the upstream boundary of the model in all scenarios, likely due to the calculation of sediment supply in

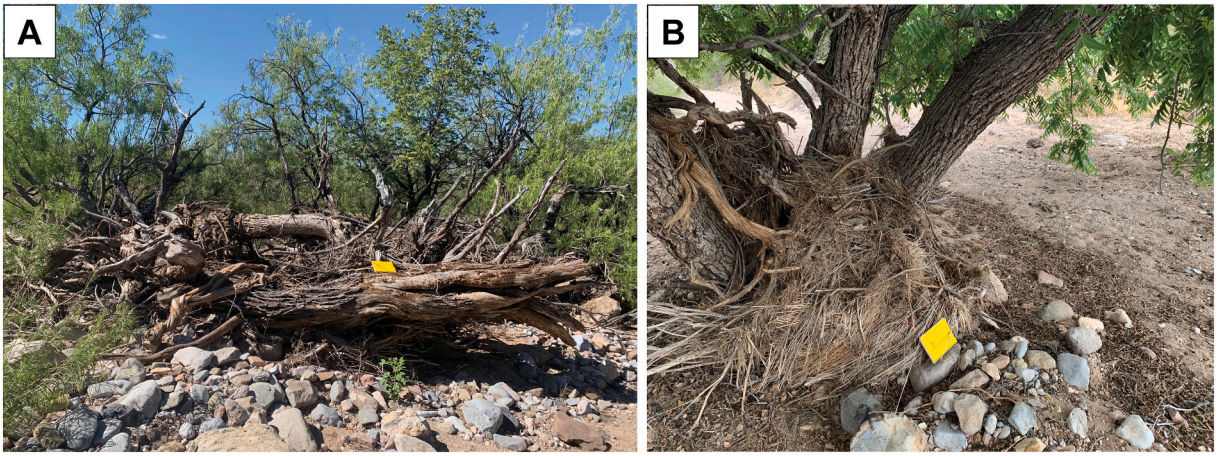

Fig. 3. Examples of LW jams in Walnut Gulch Experimental Watershed. Flow is into the image (A) and from right to left (B).

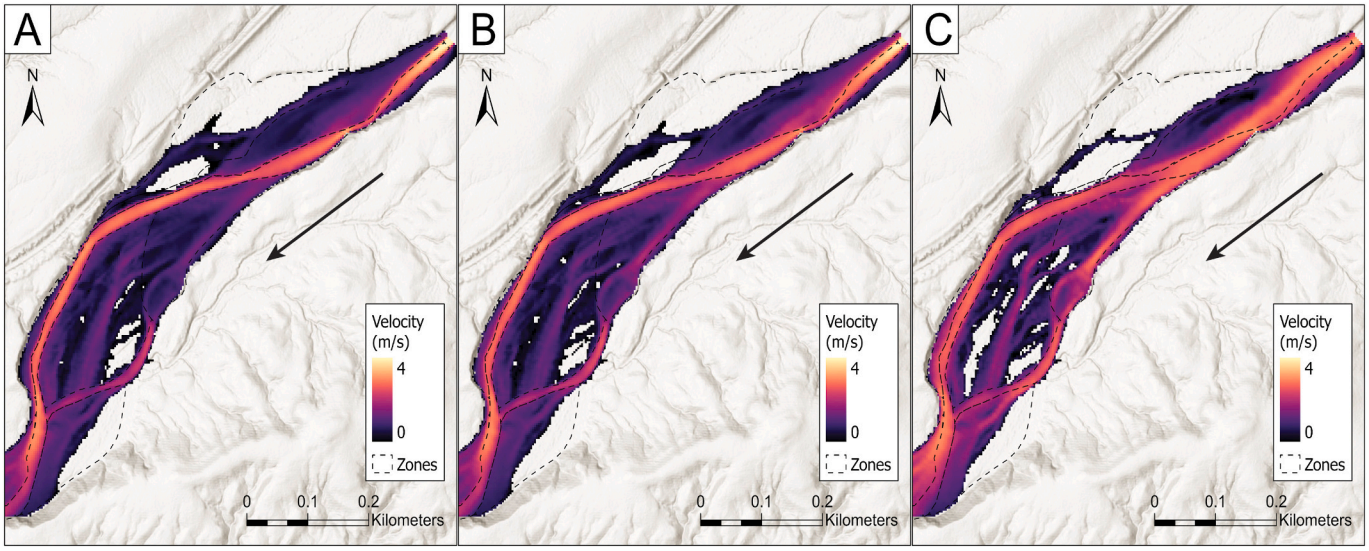

Fig. 4. Velocity at peak discharge (timestep = 2 h) for the calibrated jam model (A), the no-jam experiment (B), and the no-vegetation experiment (C). Arrow indicates direction of flow.

Table 2
Mean velocity and standard deviation of velocity in each model region at peak discharge ($t = 2$ h) for each modeled scenario. Percent change in mean velocity is calculated based on the calibrated jam model.

Model region	Scenario	Mean velocity (m/s) [% change]	Standard deviation (m/s)
Channel	Jams	2.46	0.63
	No jams	2.46 [+0 %]	0.61
	No veg	2.37 [−0.1 %]	0.43
Floodplain	Jams	0.86	0.46
	No jams	0.85 [−0.1 %]	0.47
	No veg	1.16 [+35 %]	0.66
Jam Region	Jams	0.93	0.46
	No jams	1.19 [+28 %]	0.54
	No veg	1.62 [+74 %]	0.77

the absence of a known sediment discharge which results in significant entrainment and subsequent deposition at the upstream boundary. The upstream-most 150 m (~10 channel widths) of the modeling domain were excluded from sediment volume calculations, to ensure entrance effects were not skewing results. Entrance effects appear to only influence the upstream-most ~100 m of the modeled reach. However, by excluding the upstream-most 150 m, we ensure that sediment transport has equilibrated, and entrance effects are not skewing results. As with changes in hydrologic characteristics, changes in morphology over the course of the runoff event were similar between the calibrated model and the no-jam experiment (Fig. 5A). Jams in the calibrated model resulted in more channel erosion (on the order of 0.1 m) and more (0.1–0.3 m) floodplain deposition (Fig. 6A & B). However, volumes of eroded and deposited sediment were comparable between the calibrated model and no-jam experiment (Table 3). The volume of eroded and deposited sediment was calculated for each run by comparing the final bed configuration ($t = 8$ h) to the initial bed elevation. Net change in sediment storage was similar between the calibrated model and no-jam experiment, with one notable exception being that the calibrated model resulted in more deposition in the jam zone than the no-jam experiment (Table 3).

In contrast, the differences between the no-jam experiment and the no-vegetation experiment are larger (Fig. 5B). The removal of vegetation resulted in less net channel erosion and less net floodplain deposition compared to the vegetated runs (calibrated model and no-jam experiment; Table 3). Higher volumes of erosion outside the channel in the no-vegetation experiment were also coupled with higher rates of deposition, resulting in comparable net change to the vegetated experiments,

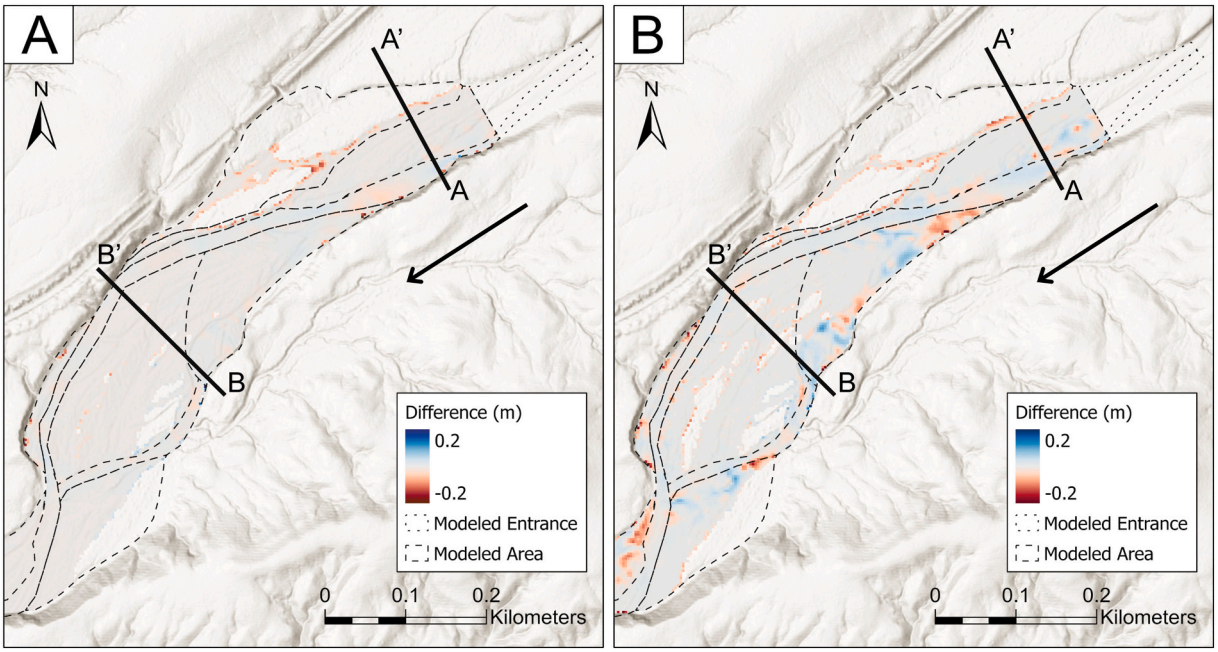

Fig. 5. Differences in elevation at peak discharge (timestep = 2 h) between the calibrated jam model and no-jam experiment (A) and no-jam experiment and no-vegetation experiment (B). Negative values indicate erosion with the removal of jams (A) or vegetation (B). Arrow indicates direction of flow.

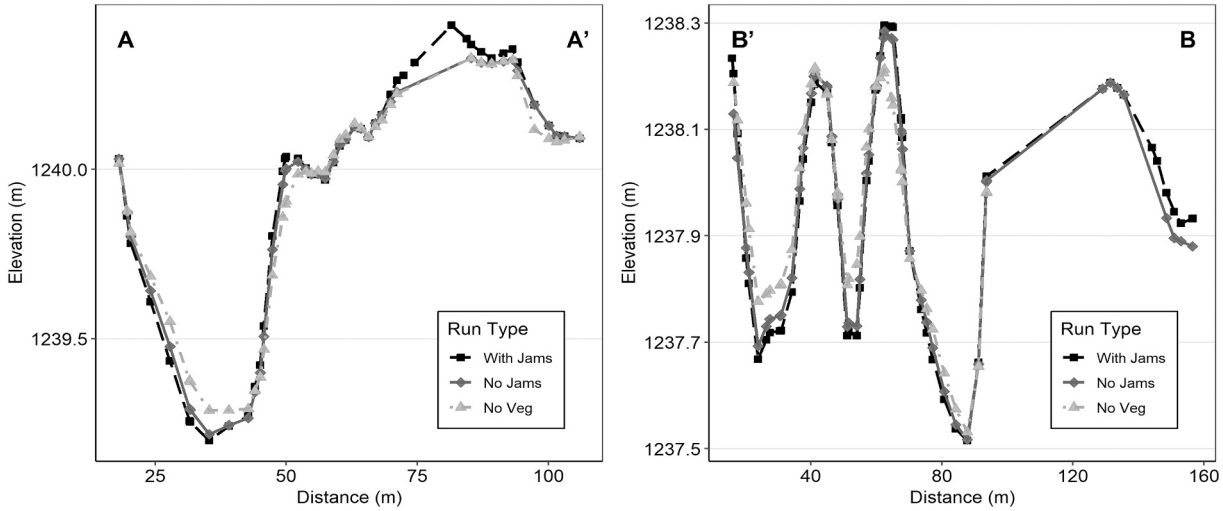

Fig. 6. Elevation cross-sections at peak runoff (timestep = 2 h) at two locations within the study area. Cross-section locations are shown in Fig. 5.

Table 3
Total volume of erosion, deposition, and net change in each model region for each modeled scenario as well as the percentage of the study area in each region experiencing erosion or deposition. Values reflect final model configuration (t = 8 h).

Model region	Scenario	Erosion (m^3)	Deposition (m^3)	Erosion (% area)	Deposition (% area)	Net change (m^3)
Channel	Jams	−474	208	59	39	−266
	No jam	−456	180	54	45	−276
	No veg	−416	250	51	48	−165
Floodplain	Jams	−39	235	24	45	+196
	No jam	−36	235	20	47	+199
	No-vegetation experiment	−178	358	22	39	+180
Jam region	Jams	−72	331	32	66	+260
	No jam	−47	282	31	66	+235
	No veg	−241	484	36	58	+244

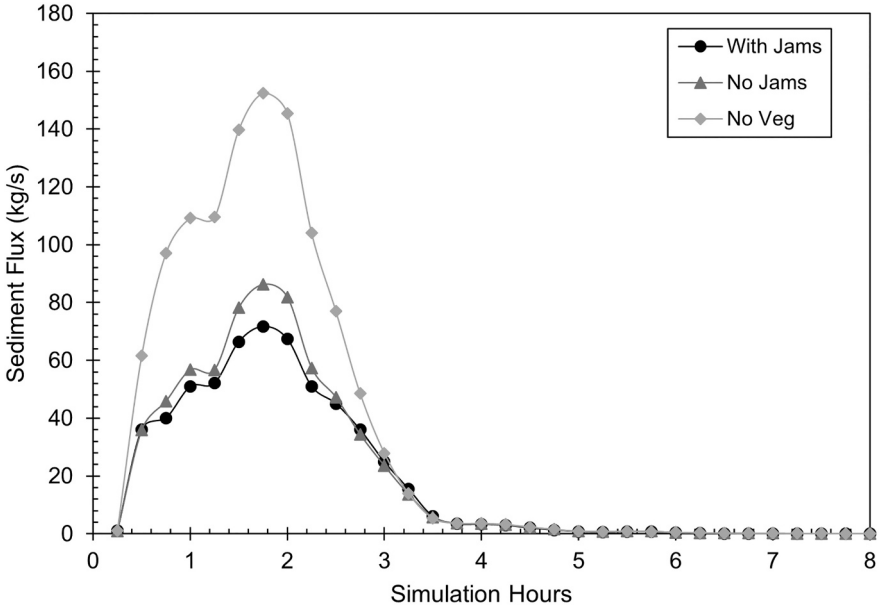

Fig. 7. Time series of sediment flux at cross-section A-A′ for the calibrated model (with jams), no-jam experiment (no jams), and no-vegetation experiment (no veg).

despite greater sediment instability (Table 3). High rates of deposition are likely due to a higher calculated sediment flux in the no-vegetation experiment (Fig. 7), which may be a result of increased sediment mobility due to higher velocities in the jam and floodplain regions of the model (Table 2). Overall, the no-vegetation experiment resulted in shallower and slightly narrower channels and lower floodplains than the vegetated scenarios (Fig. 6).

5. Discussion

5.1. Patterns of erosion and deposition with LW and vegetation

Vegetation and LW worked in tandem to effectively confine flow, resulting in high velocity in the main channel in the calibrated jam scenario. However, the basic template of channel change – wider and deeper channels – is likely driven by the roughness of vegetation in the Walnut Gulch study reach, based on the more substantial changes between the vegetated scenarios and the no-vegetation experiment (Figs. 5 & 6). The additional roughness of jams on top of vegetation resulted in minor (±0.1–0.3 m) enhancement of floodplain deposition and channel scour while still resulting in similar post-flood topography (Fig. 6).

Although the inclusion of jams still resulted in net sediment storage in the floodplain and throughout the reach, the added roughness of jams resulted in increased erosion in the channel (Table 3). The effect of jams increasing sediment transport and scour due to flow concentration has been shown in prior field (Keller and Swanson, 1979; Abbe and Montgomery, 2003) and modeling studies (Cherry and Beschta, 1989; Schalko et al., 2019) for sand-bed perennial rivers. Greater channel erosion was also coupled with greater channel deposition in the calibrated jam model compared to the no-jam experiment, which is consistent with prior studies that document significant deposition upstream of LW accumulations in perennial rivers (Bilby, 1981; Nakamura and Swanson, 1993; Abbe and Montgomery, 2003; Faustini and Jones, 2003; Short et al., 2015). However, the result of net channel erosion even in the calibrated jam model is likely a result of the location of LW in our study area. Only 6 % of jams were found in the channel, whereas previous studies have focused on the effect of sediment deposition around in-channel LW. In contrast, our study found the majority (94 %) of jams outside of the channel region, where few studies have documented the magnitude of sediment deposition behind or around LW accumulations during floods. For example, in forested perennial streams in England, Jeffries et al. (2003) documented ~0.5 m of deposition associated with LW jams, and Sear et al. (2010) measured up to 0.16 m of sedimentation behind LW accumulations annually. Based on these comparisons with humid perennial floodplains, jams in the calibrated model resulted in similar magnitudes of additional sedimentation on the floodplain in Walnut Gulch (Fig. 6A).

In dryland ephemeral streams, field studies have also found that riparian vegetation can increase in-channel velocity and drive scour in main and secondary channels during large floods (Graeme and Dunkerley, 1993; Wende and Nanson, 1998; Merritt and Wohl, 2003). Therefore, similarities in topography and net erosion/deposition between the two vegetated scenarios (the jam model and no-jam experiment) are expected, given that both LW and vegetation result in similar channel change. The result of vegetation driving channel morphology is also expected, given that vegetation covers ~31 % of the reach area compared to 0.1 % of area covered by jams and that 91 % of jams were deposited in association with vegetation.

In the no-vegetation experiment, increased velocity on the floodplain and decreased velocity within the main channel facilitated significant sediment deposition outside of the channel region (Table 3). Significant sediment deposition has been recorded in wide or braided perennial and ephemeral dryland streams during high magnitude, long recurrence interval floods due to a loss of transport capacity (e.g., Friedman et al., 1996; Merritt and Wohl, 2003). As we shift roughness values in the no-vegetation experiment to mimic those of the channel across the entire reach, there is ample energy available to transport sediment-laden flows into the floodplain where energy dissipates and sediment is deposited, suggesting topography itself is a significant factor influencing sedimentation in ephemeral streams. Smaller magnitude flows that are confined to a single, narrower channel can subsequently erode sediment deposited during larger floods (e.g., Friedman et al., 1996). However, given a decrease in transport capacity in wide, braided ephemeral reaches during large flows, we may expect significant amounts of LW and CPOM deposition as well from upstream vegetated areas in the watershed. LW and CPOM can trap moisture and stabilize sediment, providing prime locations for seedling establishment (Pettit et al., 2005), thus increasing the vegetated area. Increased vegetation would provide increased LW inputs – due to falling limbs or tree mortality – and create future trapping sites for new LW accumulations. As shown in this study, LW enhances the process of floodplain deposition and channel scour created by vegetation. Therefore, deposition associated with a no-

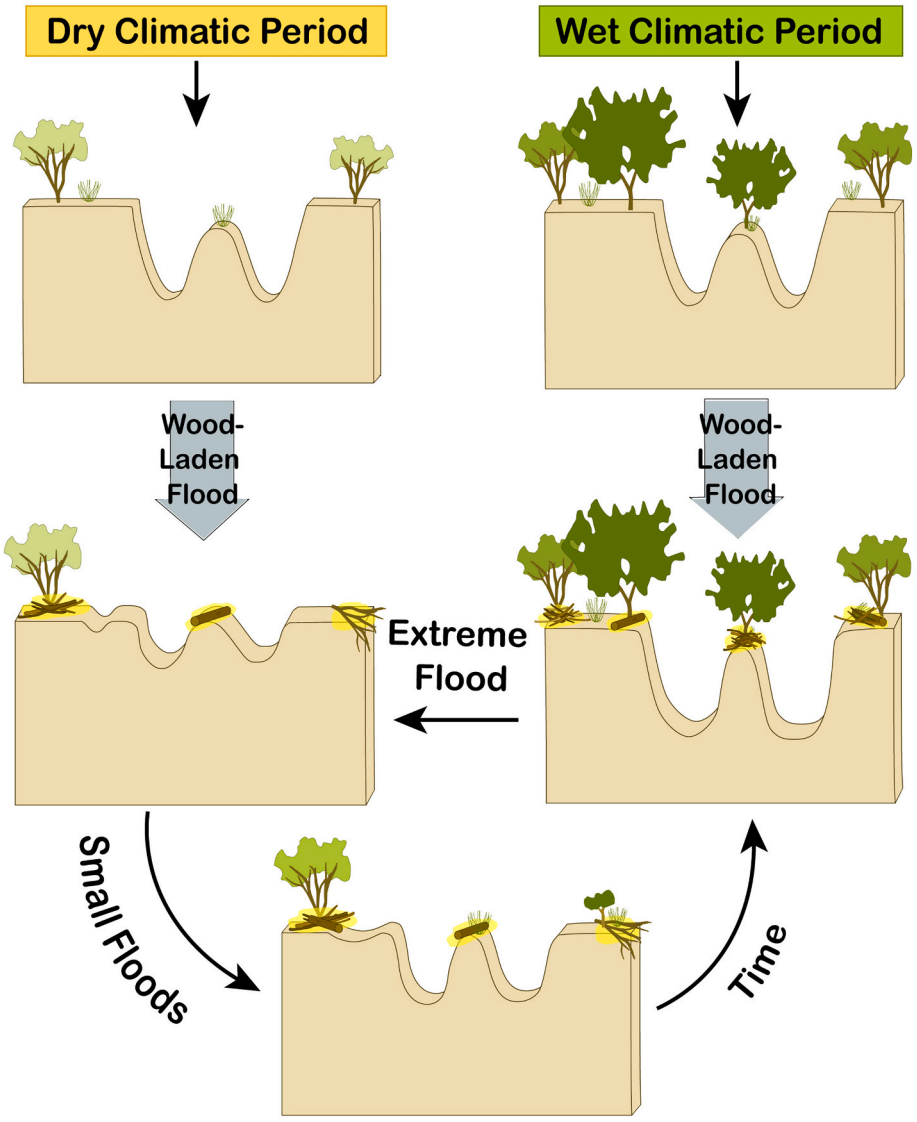

Fig. 8. Conceptual diagram showing deposition potential and channel change following a moderate, wood-laden flood. Under wet climatic conditions with healthy vegetation, large wood would be trapped on woody vegetation, leading to increased riparian roughness and deeper and wider channels. Under dry climatic conditions, where vegetation has begun to die back and riparian roughness is low, runoff would likely spread evenly across the reach, resulting in massive deposition. In this scenario, deposition of large wood and CPOM could provide sites of increased moisture and nutrients for seedling establishment, thus encouraging vegetation growth. Over time and subsequent small floods, this could provide positive feedback leading to denser and healthier vegetation. Extreme floods could uproot vegetation and reset the reach.

vegetation scenario could eventually lead to channel erosion during floods, as LW facilitates a transition back to a vegetated scenario further stabilized by jams (Fig. 8).

The scenario of an unvegetated floodplain and wide, sandy channel is not unfamiliar in the lower reaches of Walnut Gulch. Aerial imagery and cross-sectional topographic surveys from the mid-20th century show that the reach upstream of Flume 1 was largely unvegetated, with a much wider channel corridor. Vegetation density has increased throughout the reach since the 1930s, concurrent with a decrease in the magnitude of annual peak discharges and increase in precipitation during non-summer months (Nichols et al., 2002; Nichols et al., 2005). The reach upstream of Flume 1 is particularly susceptible to channel change due to a lack of confinement. The main stem of Walnut Gulch is longitudinally variable with several reaches that are bedrock confined and fault aligned. Confined reaches cannot readily migrate laterally and stand in contrast to floodplain type reaches – such as upstream of Flume 1 – where runoff can expand laterally, and channel morphology can vary significantly over timescales of single storms to decades.

Unconfined dryland streams in general go through wet and dry phases, with morphology based on climate (Burkham, 1972; Graf, 1988). Wet phases are defined by years to decades of above average precipitation, while dry phases are characterized by below average precipitation. (Nanson and Croke, 1992; Manners et al., 2014). During wet phases, vegetation thrives, and more frequent moderate to low magnitude floods do not readily remove vegetation or rework the floodplain. Dry phases result in vegetation dieback, and intermittent moderate to large floods are able to significantly erode the channel and floodplain, effectively widening the unvegetated channel. In either phase, a sufficiently large flood may reset the river corridor by removing vegetation and widening the channel (Friedman et al., 1996; Friedman and Lee, 2002). Increased vegetation density upstream of Flume 1 in WGEW since the 1930s – concurrent with increased precipitation in the watershed –has led to effective channel narrowing, with the development of more expansive vegetated floodplains (Nichols et al., 2005). Although our models suggest that the 2017 flood was large enough to widen the channel, stability provided by vegetation and enhanced by jams prevented topographic reset in the form of significant erosion or deposition. Our study reach therefore provides an example of the stability provided by vegetation and LW in ephemeral streams during relatively wet climatic periods (Fig. 8).

5.2. *Modeling limitations*

Modeling results can be explained and supported by prior field studies in both perennial and ephemeral dryland watersheds, suggesting that the model outputs are reasonable and interpretable. Given the

traditional difficulty in collecting data during flash floods (Borga et al., 2014), a modeling approach can provide the benefit of a first-order approximation of the morphodynamic influence of LW in an ephemeral stream, compared to the more well-known influence of vegetation. Still, limited field data prevent the models presented in this study from being fully validated with other flow events, meaning that model parameters could not be applied to a different discharge event or watershed without further calibration. Additionally, the scale at which modeling can be conducted is dependent on the scale of topographic inputs and computational power. To reduce complexity in the model, jams were estimated by generally increasing roughness in large areas of concentrated jam deposition, which is consistent with hydrological models developed for LW in perennial rivers (Addy and Wilkinson, 2019). However, the surface area covered by jams is minimal in Walnut Gulch, and the influence of individual LW jams (particularly local sedimentation and scour) occurs on too fine a scale to be captured by this model. Instead, our model represents potential reach-scale changes which can have implications for macro-scale sediment transport and river corridor morphology. Future studies monitoring the persistence of LW jams and high-resolution sedimentation and erosion around LW in ephemeral streams could provide more insight into micro-scale geomorphic changes and habitat associate with jams and LW.

5.3. Impact of sediment dynamics on dryland ecosystems

The majority of rivers globally are non-perennial (Messager et al., 2021), and in the American Southwest, up to 80 % of the river network is estimated to be ephemeral or intermittent (Levick et al., 2008). Ephemeral streams are important sources of water, nutrients, and sediment to downstream perennial rivers and waterbodies (Goodrich et al., 2018). Excess sediment delivery from ephemeral streams can have a negative impact on water quality, waterway health, and reservoir sedimentation (Sandercock and Hooke, 2011). However, sediment is also a necessary resource for the creation of key fluvial features (i.e., bars, which are useful for both recreation and habitat) and for the creation of fresh alluvial surfaces necessary for the establishment of many riparian trees (Hupp and Osterkamp, 1996; Kemper et al., 2021). Ultimately, the balance between storage and erosion of sediment from ephemeral streams such as Walnut Gulch can have important implications for downstream ecosystems and watershed-scale management.

Local erosion and deposition can affect vegetation health and habitat within a reach. Sediment deposition is necessary for the establishment of many riparian pioneer species, but excess sedimentation can cause tree mortality and limit seedling survival (Levine and Stromberg, 2001; Kui and Stella, 2016). Erosion can prevent vegetation burial, but excess scour can uproot and remove vegetation (Rominger et al., 2010). Therefore, the balance between erosion and deposition matters for local, reach-scale ecosystems as well.

The calibrated jam model was more stable (resulted in lower volumes of erosion and sedimentation) than the no-vegetation experiment, yet more active (greater net sediment accumulation) than the no-jam experiment (Table 3), suggesting that jams could help maintain the balance between scour and deposition that supports local and downstream ecosystems in ephemeral watersheds. Sediment stability around LW and CPOM jams can additionally support biota. LW and CPOM accumulations are relatively stable compared to mobile, sandy beds and can retain moisture for longer post-flow, thus providing valuable habitat for aquatic invertebrates (Ward et al., 1982; Chester and Robson, 2011). On floodplains and surfaces inundated less frequently, LW and CPOM piles can also be colonized by lizards, rodents, and desert turtles (Buhlmann et al., 2009). Therefore, LW and CPOM jams in Walnut Gulch could provide multiple ecosystem benefits beyond impacts to channel morphology.

6. Conclusion

The presence of LW and CPOM jams in dryland ephemeral streams has been documented globally, but a quantitative assessment of the morphodynamic impact of LW has been lacking. Morphodynamic modeling provides a useful framework by which hydro- and morphodynamics can be estimated in flash flood-dominated systems, such as Walnut Gulch. Modeling revealed that LW creates similar channel changes as vegetation. Primarily, LW jams and vegetation help confine high velocity flows, leading to deeper and wider channels. The additional roughness of LW increased channel scour and floodplain deposition by ~0.1–0.3 m. Results suggest that LW jams could enhance sediment mobility in the channel and sediment stability in the floodplain along ephemeral channels, which can have implications for local and downstream ecosystems.

Declaration of competing interest

The authors declare that they have no known competing financial interests or personal relationships that could have appeared to influence the work reported in this paper.

Data availability

Data will be made available on request.

Acknowledgements

Financial support was provided by the U.S. National Science Foundation Graduate Research Fellowship Program to Scamardo. Field work was greatly assisted by multiple staff and technicians at the USDA ARS Southwest Watershed Research Center in Tucson and Tombstone, AZ. Lastly, we would like to thank the two anonymous reviewers whose comments helped improve the manuscript.

Appendix A. Supplementary data

Supplementary data to this article can be found online at https://doi.org/10.1016/j.geomorph.2022.108444.

References

Abbe, T.B., Montgomery, D.R., 2003. Patterns and processes of wood debris accumulation in the Queets River basin, Washington. Geomorphology 51, 81–107.
Addy, S., Wilkinson, M.E., 2019. Representing natural and artificial in-channel large wood in numerical hydraulic and hydrological models. WIREs Water 6 (6), e1389.
Anderson, D.C., Stricker, C.A., Nelson, S.M., 2016. Wood decay in desert riverine environments. For. Ecol. Manag. 365, 83–95.
Arcement, G.J., Schneider, V.R., 1989. Guide for selecting Manning's roughness coefficients for natural channels and floodplains. In: U.S. Geological Survey Water Supply Paper 2339. U.S. Geological Survey.
Bilby, R.E., 1981. Role of organic debris dams in regulating the export of dissolved and particulate matter from a forested watershed. Ecology 62, 1234–1243.
Borga, M., Stoffel, M., Marchi, L., Marra, F., Jakob, M., 2014. Hydrogeomorphic response to extreme rainfall in headwater systems: flash floods and debris flows. J. Hydrol. 518, 194–205.
Buhlmann, K.A., Congdon, J.D., Gibbons, J.W., Greene, J., 2009. Ecology of Chicken Turtles (Dierochelys reticularia) in a seasonal wetland ecosystem: exploiting resources and refuge environments. Herpetologica 65, 39–53.
Bunch, C.E., Forbes, B.T., 2019. 09471143 – Walnut Gulch Below ARS Flume 6, Near Tombstone, AZ – 07/28/2017 Flow Event Data: U.S. Geological Survey Data Release. 10.5066/P9O9JWPW.
Burkham, D.E., 1972. In: Channel Changes of the Gila River in Safford Valley, Arizona, 1846-1970. U.S. Geological Survey Professional Paper 655-G, p. 24.
Cherry, J., Beschta, R.L., 1989. Coarse woody debris and channel morphology: a flume study. Water Resour. Bull. 25, 1031–1036.
Chester, E.T., Robson, B.J., 2011. Drought refuges, spatial scale and recolonisation by invertebrates in non-perennial streams. Freshw. Biol. 56 (10), 2094–2104.
Collins, B.D., Montgomery, D.R., Fetherston, K.L., Abbe, T.B., 2012. The floodplain large wood cycle hypothesis: a mechanism for the physical and biotic structing of temperate forested alluvial valleys in the North Pacific coastal ecoregion. Geomorphology 139–140, 460–470.

Cowan, W.L., 1956. Estimating hydraulic roughness coefficients. Agric. Eng. 37, 473–475.
Curran, J.H., Wohl, E.E., 2003. Large woody debris and flow resistance in step-pool channels, Cascade Range, Washington. Geomorphology 51, 141–157.
Dunkerley, D., 2014. Nature and hydro-geomorphic roles of trees and woody debris in a dryland ephemeral stream: Fowlers Creek, arid western New South Wales, Australia. J. Arid Environ. 102, 40–49.
Engelund, F., Hansen, E., 1972. A Monograph on Sediment Transport in Alluvial Streams. Technical Press, Copenhagen.
Faustini, J.M., Jones, J.A., 2003. Influence of large woody debris on channel morphology and dynamics in steep, boulder-rich mountain streams, western Cascades, Oregon. Geomorphology 51, 187–205.
Friedman, J.M., Lee, V.J., 2002. Extreme floods, channel change, and riparian forests along ephemeral streams. Ecol. Monogr. 72, 409–425.
Friedman, J.M., Osterkamp, W.R., Lewis Jr., W.M., 1996. The role of vegetation and bed-level fluctuations in the process of channel narrowing. Geomorphology 14, 341–351.
Galia, T., Skarpich, V., Tichavsky, R., Vardakas, L., Silhan, K., 2018. Longitudinal distribution and parameters of large wood in a Mediterranean ephemeral stream. Geomorphology 310, 15–28.
Galia, T., Horacek, M., Macurova, T., Skarpich, V., 2019. Drivers of low instream large wood retention and imprints of wood mobility in mountain nonperennial streams of a Mediterranean semi-arid environment. Water Resour. Res. 55, 7843–7859.
Galia, T., Macurova, T., Vardakas, L., Skarpich, V., Matuskova, T., Kalogianni, E., 2020. Drivers of variability in large wood loads along the fluvial continuum of a Mediterranean intermittent river. Earth Surf. Process. Landf. 45 (9), 2048–2062.
Goodrich, D.C., Kepner, W.G., Levick, P.J., Wiginton Jr., P.J., 2018. Southwestern intermittent and ephemeral stream connectivity. J. Am. Water Resour. Assoc. 54, 400–422.
Graeme, E., Dunkerley, D.L., 1993. Hydraulic resistance by the river red gum, Eucaluptus camaldulensis, in Ephemeral Desert Streams. Aust. Geogr. Stud. 31, 141–154.
Graf, W.L., 1988. Fluvial Processes in Dryland Rivers. Springer-Verlag, Berlin, New York.
Gurnell, A.M., 2013. Wood in fluvial systems. In: Wohl, E. (Ed.), Treatise on Geomorphology, Fluvial Geomorphology, vol 9. Academic Press, San Diego, CA, pp. 163–188.
Gurnell, A., Tockner, K., Edwards, P., Petts, G., 2005. Effects of deposited wood on biocomplexity of river corridors. Front. Ecol. Environ. 3, 377–382.
Harvey, J., Gooseff, M., 2015. River corridor science: hydrologic exchange and ecological consequences from bedforms to basins. Water Resour. Res. 51 (9), 6893–6922.
Heilman, P., Nichols, M.H., Goodrich, D.C., Miller, S.N., Guertin, D.P., 2008. Geographic information systems database, Walnut Gulch experimental watershed, Arizona, United States. Water Resour. Res. 44, W05S11.
Hupp, C.R., Osterkamp, W.R., 1996. Riparian vegetation and fluvial geomorphic processes. Geomorphology 14, 277–295.
Jacobson, P.J., Jacobson, K.M., Angermeier, P.L., Cherry, D.S., 1999. Transport, retention, and ecological significance of woody debris within a large ephemeral river. J. N. Am. Benthol. Soc. 18 (4), 429–444.
Jeffries, R., Darby, S.E., Sear, D.A., 2003. The influence of vegetation and organic debris on floodplain sediment dynamics: case study of a low-order stream in the New Forest, England. Geomorphology 51, 61–80.
Keller, E.A., Swanson, F.J., 1979. Effects of large organic material on channel form and fluvial processes. Earth Surf. Process. 4, 361–380.
Kemper, J.T., Thaxton, R.D., Rathburn, S.L., Friedman, J.M., Mueller, E.R., Scott, M.L., 2021. Sediment-ecological connectivity in a large river network. Earth Surf. Process. Landf. 47, 639–657.
Klaar, M.J., Maddock, I., Milner, A.M., 2009. The development of hydraulic and geomorphic complexity in recently formed streams in Glacier Bay National Park, Alaska. River Res. Appl. 25, 1331–1338.
Kui, L., Stella, J.C., 2016. Fluvial sediment burial increases mortality of young riparian trees but induces compensatory growth response in survivors. For. Ecol. Manag. 366, 32–40.
Lai, Y.G., 2010. Two-dimensional depth-averaged flow modeling with an unstructured hybrid mesh. J. Hydraul. Eng. 136, 12–23.
Lai, Y.G., 2020. A two-dimensional depth-averaged sediment transport mobile-bed model with polygonal meshes. Water 12, 1032.
Lassettre, N.S., Piegay, H., Dufour, S., Rollet, A.J., 2008. Decadal changes in distribution and frequency of wood in a free meandering river, the Ain River, France. Earth Surf. Process. Landf. 33, 1098–1112.
Levick, L., Fonseca, J., Goodrich, D., Hernandex, M., Semmens, D., Leidy, R., Scianni, M., Guertin, P., Tluczek, M., Kepner, W., 2008. The Ecological and Hydrological Significance of Ephemeral and Intermittent streams in the arid and semi-arid American Southwest. EPA/600/R-08/134 and ARS/233046. U.S. Environmental Protection Agency, Office of Research and Development and USDA/ARS Southwest Watershed Research Center, Washington, D.C.
Levine, C.M., Stromberg, J.C., 2001. Effects of flooding on native and exotic plant seedlings: implications for restoring south-western riparian forests by manipulating water and sediment flows. J. Arid Environ. 49, 111–131.
Lininger, K.B., Scamardo, J.E., Guiney, M.R., 2021. Floodplain large wood and organic matter jam formation after a large flood: investigating the influence of floodplain forest stand characteristics and river corridor morphology. Journal of Geophysical Research: Earth Surface 126, e2020JF006011.
Livers, B., Lininger, K.B., Kramer, N., Sendrowski, A., 2020. Porosity problems: comparing and reviewing methods for estimating porosity and volume of wood jams in the field. Earth Surf. Process. Landf. 45, 3336–3353.
Lotsari, E.S., Calle, M., Benito, G., Kukko, A., Kaartinen, H., Hyyppa, J., Hyyppa, H., Alho, P., 2018. Topographical change caused by moderate and small floods in a gravel bed ephemeral river – a depth-averaged morphodynamic simulation approach. Earth Surface Dynamics 6, 163–185.
MacFarlane, W.A., Wohl, E., 2003. Influence of step composition on step geometry and flow resistance in step-pool streams of the Washington Cascades. Water Resour. Res. 39, 1037.
Manners, R.B., Doyle, M.W., Small, M.J., 2007. Structure and hydraulics of natural woody debris jams. Water Resour. Res. 43, W06432.
Manners, R.B., Schmidt, J.C., Scott, M.L., 2014. Mechanisms of vegetation -induced channel narrowing of an unregulated canyon river: results from a natural field-scale experiment. Geomorphology 211, 100–115.
Merritt, D.M., Wohl, E.E., 2003. Downstream hydraulic geometry and channel adjustment during a flood along an ephemeral arid-region drainage. Geomorphology 52, 165–180.
Messager, M.L., Lehner, B., Cockburn, C., Lamouroux, N., Pella, H., Snelder, T., Tockner, K., Trautmann, T., Watt, C., Datry, T., 2021. Global prevalence of non-perennial rivers and streams. Nature 594, 391–397.
Meyer-Peter, E., Muller, R., 1948. Formulas for bed-load transport. In: Proceedings, International Association for Hydro-environment Engineering and Research, 2nd Meeting: Stockholm, Sweden.
Michaelides, K., Hollings, R., Singer, M.B., Nichols, M.H., Nearing, M.A., 2018. Spatial and temporal analysis of hillslope-channel coupling and implications for the longitudinal profile in a dryland basin. Earth Surf. Process. Landf. 43 (8), 1608–1621.
Montgomery, D.R., Abbe, T.B., 2006. Influence of logjam-formed hard points on the formation of valley-bottom landforms in an old-growth forest valley, Queets River, Washington, USA. Quat. Res. 65, 147–155.
Montgomery, D.R., Collins, B.D., Buffington, J.M., Abbe, T.B., 2003. Geomorphic effects of wood in rivers. In: Gregory, S.V., Boyer, S.L., Gurnell, A.M. (Eds.), The Ecology and Management of Wood in World Rivers. American Fisheries Society Symposium 37. American Fisheries Society, Bethesda, M.D., pp. 21–47
Nakamura, F., Swanson, F.J., 1993. Effects of coarse woody debris on morphology and sediment storage of a mountain stream system in western Oregon. Earth Surf. Process. Landf. 18, 43–61.
Nanson, G.C., Croke, J.C., 1992. A genetic classification of floodplains. Geomorphology 4, 459–486.
Nepf, H.M., 1999. Drag, turbulence, and diffusion in flow through emergent vegetation. Water Resour. Res. 35, 479–489.
Nichols, M.H., Renard, K.G., Osborn, H.B., 2002. Precipitation changes from 1956 to 1996 on the Walnut Gulch Experimental Watershed. J. Am. Water Resour. Assoc. 38, 161–172.
Nichols, M.H., Nearing, M., Shipek, C., 2005. Trends in precipitation, runoff, and in-channel vegetation on the USDA-ARS Walnut Gulch Experimental Watershed. In: Proceedings, World Water and Environmental Resources Congress. American Society of Civil Engineers, Anchorage, Alaska.
Osterkamp, W.R., 2008. Geology, soils, and geomorphology of the Walnut Gulch Experimental Watershed, Tombstone Arizona. J. Ariz. Nev. Acad. Sci. 40 (2), 136–154.
Pettit, N.E., Naiman, R.J., Rogers, K.H., Little, J.E., 2005. Post-flooding distribution and characteristics of large woody debris piles along the semi-arid Sabie River, South Africa. River Res. Appl. 21 (1), 27–38.
Rominger, J.T., Lightbody, A.F., Nepf, H.M., 2010. Effects of added vegetation on sand bar stability and stream hydrodynamics. J. Hydraul. Eng. 136, 994–1002.
Ruiz-Villanueva, V., Piégay, H., Gurnell, A.M., Marston, R.A., Stoffel, M., 2016. Recent advances quantifying the large wood dynamics in river basins: new methods and remaining challenges. Rev. Geophys. 54, 611–652.
Sandercock, P.J., Hooke, J.M., 2011. Vegetation effects on sediment connectivity and processes in an ephemeral channel in SE Spain. J. Arid Environ. 75, 239–254.
Schalko, I., Lageder, C., Schmocker, L., Weitbrecht, V., Boes, R.M., 2019. Laboratory flume experiments on the formation of spanwise large wood accumulations: Part II – Effects on local scour. Water Resour. Res. 55, 4871–4885.
Scott, S., 2006. Predicting Sediment Transport Dynamics in Ephemeral Channels: A Review of Literature. ERDC/CHL CHETN-VII-6, Vicksburg, MS: U.S. Army Engineer Research and Development Center. http://chl.erdc.usace.army.mil/chetn/.
Sear, D.A., Millington, C.E., Kitts, D.R., Jeffries, R., 2010. Logjam controls on channel: floodplain interactions in wooded catchments and their role in the formation of multi-channel patterns. Geomorphology 116, 305–319.
Shields, F.D., Smith, R.H., 1992. Effects of large woody debris removal on physical characteristics of a sand-bed river. Aquat. Conserv. Mar. Freshwat. Ecosyst. 2 (2), 145–163.
Short, L.E., Gabet, E.J., Hoffman, D.F., 2015. The role of large woody debris in modulating the dispersal of a post-fire sediment pulse. Geomorphology 246, 351–358.
Smith, R.E., Chery, D.L., Renard, K.G., Gwinn, W.R., 1981. Supercritical flow flumes for measuring sediment-laden flow. In: U.S. Department of Agriculture Technical Bulletin No. 1655, 72 p.
Swanson, F.J., Gregory, S.V., Iroume, A., Ruiz-Villanueva, V., Wohl, E., 2021. Reflections on the history of research on large wood in rivers. Earth Surf. Process. Landf. 46, 55–66.
Ward, J.V., Zimmerman, H.J., Cline, L.D., 1982. Lotic zoobenthos of the Colorado River system. In: Fontane, T.D., Bartell, S.M. (Eds.), Dynamics of Lotic Ecosystems, Stroudsburg, Downden, Hutchinson, and Ross.
Wende, R., Nanson, G.C., 1998. Anabranching rivers: ridge-form alluvial channels in tropical northern Australia. Geomorphology 22, 205–224.
Wheaton, J.M., Brasington, J., Darby, S.E., Sear, D.A., 2010. Accounting for uncertainty in DEMs from repeat topographic surveys: improved sediment budgets. Earth Surf. Process. Landf. 35, 136–156.

Wohl, E., 2011. Threshold-induced complex behavior of wood in mountain streams. Geology 39, 587–590.
Wohl, E., 2017. Bridging the gaps: an overview of wood across time and space in diverse rivers. Geomorphology 279, 3–26.
Wohl, E., Scamardo, J., 2022. Patterns of organic matter accumulation in dryland river corridors of the southwestern United States. Sci. Total Environ. 833, 155136.
Wohl, E., Scott, D.N., 2017. Wood and sediment storage and dynamics in river corridors. Earth Surf. Process. Landf. 42, 5–23. https://doi.org/10.1002/esp.3909.
Wohl, E., Cadol, D., Pfeiffer, A., Jackson, K., Laurel, D., 2018. Distribution of large Wood within River Corridors in Relation to Flow Regime in the Semiarid Western US. Water Resour. Res. 54, 1890–1904.